Digest Journal of Nanomaterials and Biostructures Vol. 18, No. 4, October-December 2023, p.1179-1186

Synthesis of mixed phase morphologies of copper oxide nanoparticles using *bis*(n-benzyl-salicydenaminato)copper(II) as a precursor

T. Xaba[a,*], P. M. Shumbula[b], S. Nyembe[c], P. Tetyana[c]
[a]*Department of Biotechnology and Chemistry, Vaal University of Technology, P/Bag X021, Vanderbijlpark, South Africa*
[b]*Department of Chemistry, University of Limpopo, Private Bag X1106 Sovenga, 0727, South Africa*
[c]*Department of Science and Innovation/Mintek Nanotechnology Innovation Centre, Advanced Materials Division, Mintek, Randburg, 2125, South Africa South Africa*

A primary amine, salicylaldehyde and copper salt were combined to prepare the *bis*(N-benzyl-salicydenaminato)copper (II) complex. The copper (II) complex was then used as a precursor to synthesize mixed phase morphological copper oxide nanoparticles via thermal decomposition method using trioctylphosphine oxide as a capping molecule at different temperatures of 120, 180, and 240 ºC. The XRD patterns of copper oxide nanoparticles synthesized at lower temperatures exhibit a mixture of monoclinic structure of CuO whereas the nanoparticles synthesized at higher temperature reveals the peaks that are attributed to mainly face-centered-cubic metallic Cu. The TEM images showed spherical particles that were increasing in sizes when the temperature was raised.

(Received May 29, 2023; Accepted October 2, 2023)

Keywords: Copper oxide, Nanoparticles, Trioctylphosphine oxide (TOPO), TGA, UV-vis, PL, XRD, and TEM

1. Introduction

Metal complexes formed through the reaction of the metal ion with Schiff bases have been studied in great detail for their various applications [1–3]. Recently, copper (II) complexes derived from Schiff bases such as salicylaldehyde with different amines have been investigated [4]. The changes in the coordination geometry around copper (II) can be affected by varying the size and nature of the substituent on the N-imino of the Schiff base ligand [4–6].

The limited size and high density of the edge surface sites of the oxide nanoparticles allow them to display unique physical and chemical properties. Metal oxides exhibit metallic, semiconductor, or insulator character due to their electronic structure differences [7]. Metal oxide nanoparticles are also essential due to their applications as nano-electronics, optoelectronics, nano-sensors, nano-devices, magnetic, electrical, mechanical and thermal, information storage, and catalysis. Among numerous metal oxide materials, copper oxide has gain attention due it ability to display a wide range of valuable physical properties which includes high temperature superconductivity, spin dynamics electron, and correlation effects [8].

CuO is a black coloured material with a high absorptivity and low thermal emittance. It has a monoclinic crystal structure with bandgap between 1.2 and 1.9 eV whereas Cu_2O is brownish-red with a cubic crystal structure and a bandgap of 2.0 and 2.2 eV. CuO and Cu_2O materials are semiconductors in nature and displayed p-type characteristic due to the copper vacancies in it structure [9-11]. Several methods have been reported for the synthesis of copper oxide nanoparticles. These techniques include sol-gel technique [12], electrochemical method [13], thermal decomposition of precursors [14], chemical precipitation method [15-16], hydrothermal method [17-18], and chemical reduction method [19-21].

* Corresponding author: thokozanix@vut.ac.za
https://doi.org/10.15251/DJNB.2023.184.1179

The preparation of *bis*(N-1,2-diphenylethyl-salicydenaminato-ƙ^{2}N,O)copper (II) complex and its co-crystal containing methanol solvent molecules using a one step process was reported by Akitsu and Einaga [22]. In their investigation, it was discovered that the guest methanol molecules forced the complex to adopt a more planar coordination environment in the solid state. Salavati-Niasari and Davar reported the synthesis of copper and copper (I) oxide nanoparticles by thermal decomposition of a new precursor [14]. The optical absorption studies were used to determine the band-gap energy. Recently, we have reported the study based on the effect of temperature on the growth of Ag_2O nanoparticles and thin films from *bis*(2-hydroxy-1-naphthaldehydato)silver(I) complex by the thermal decomposition of spin–coated films. The results proved that the temperature plays a significant role in controlling nature of the nanoparticles [23].

In the present work, the synthesis of copper oxide nanoparticles by the thermal decomposition of *bis*(N-benzyl-salicydenaminato)copper (II) complex as a precursor is reported. The synthesized nanomaterials were characterized by ultraviolet–visible (UV–vis) spectroscopy, photoluminescence (PL), X-ray diffraction (XRD), and transmission electron microscopy (TEM).

2. Experimental

2.1. Materials

Salicylaldehyde, benzamide, copper acetate monohydrate and trioctylphosphine oxide (TOPO) were purchased from Sigma-Aldrich. Methanol, ethanol, and toluene were reagents purchased from Merck chemicals and were all used without further purification.

2.2. Preparation of the Bis(N-benzyl-salicydenaminato)copper (II) complex

The complex was produced using the reported procedure [23, 24]. Briefly, an equimolar of benzamine (10 mmol) was added into salicylaldehyde (10 mmol) in methanol followed by the addition of copper (II) acetate (5 mmol) in methanol into a 100 mL two necked flask. The mixture was refluxed at a temperature of 50 ^oC for 3 hrs. The formed precipitate was filtered, washed three times with ethanol and dried in a desiccator. *The product was obtained as a* very dark brown solid, *m.pt. 247 ^oC, CHN analysis: Calc.: C, 68.47; H, 4.43; N, 6.14; O, 7.15. Found: C, 68.26; H, 4.40; N, 6.08; O, 7.09. Significant FTIR bands: ν(C=N): 1608 cm^{-1}, ν(C-O): 1329 cm^{-1}, ν(Cu-O): 521 cm^{-1}, ν(Cu-N): 401 cm^{-1}.*

2.3. Synthesis of TOPO capped copper oxide nanoparticles

Copper oxide nanoparticles were prepared by thermal decomposition of *bis*(N-benzyl-salicydenaminato)copper (II) complex in trioctylphosphine oxide (TOPO). In a typical reaction, TOPO (5 g) was mixed with the copper precursor (0.5 g) in a two necked flask. The mixture was refluxed and heated to 120 °C under nitrogen environment. The temperature was maintained for an hour. The mixture was then allowed to cool to a temperature of about 70 °C. An addition of methanol (30 mL) produced a reddish brown precipitate which was separated by centrifugation. The product was washed three times with methanol and re-dispersed in toluene for characterisation. To study the effect of temperature, the procedure was repeated with a temperature of 180 and 240 °C.

2.4. Physical measurements

Elemental analysis was performed using a Perkin-Elmer automated model 2400 series II CHNS/O analyzer. FTIR spectrum was done in the range 400–4000 cm^{-1} through the utilization of a Bruker FTIR tensor 27 spectro-photometer. A Perkin-Elmer Pyris 6 TGA was used for thermogravimetric analysis. It was conducted at a 20 °C min^{-1} heating rate from 30 up to 900 °C in a closed perforated aluminium pan under nitrogen gas. UV-Vis absorption measurements of the copper oxide nanoparticles were carried out using a Perkin-Elmer Lambda 1050 UV/vis/NIR spectrometer while an Edinburgh Instruments FLS920 spectrofluorimeter was used to study photoluminescence properties of the particles. The quartz cuvettes (1 cm path length) were used to

carry the solution using toluene as a solvent. Transmission electron microscopy (TEM) was conducted using a Tecnai F30 FEG TEM instrument at an accelerating voltage of 300 kV. Samples for morphological analysis were prepared by placing 1 or 2 drop of the copper oxide nanoparticles on a lacey carbon copper grids which was previously dissolved in toluene. X-ray diffraction patterns were collected on a Bruker AXS D8 diffractometer using Cu-Karadiation where the samples were set flat and scanned between 2θ = 20-90º.

3. Results

The chemical reaction between salicylaldehyde, amine and $Cu(CH_3COO)_2.H_2O$ in methanol at a temperature of 50 °C produced *bis*(N-benzyl-salicydenaminato)copper (II) complex as shown in Scheme 1.

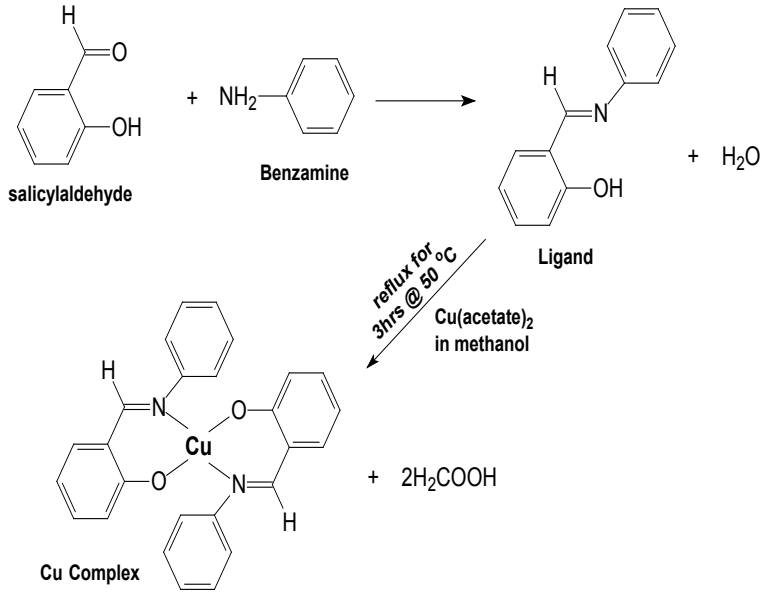

Scheme 1. Preparation of bis(N-benzyl-salicydenaminato)copper (II) complex.

3.1. Structural properties of the copper complex

The FTIR spectrum of bis(N-benzyl-salicydenaminato)copper (II) complex in Figure 1(a) exhibits a strong band at 1602–1608 cm^{-1} that is due to νC=N vibration of the imine. The presence of νC=N in the complex at a lower frequency is due to the decrease in electron density in the azomethine linkage which is a proof that C=N has been coordinated to the metal centre. A strong band was observed at 1329–1176 cm^{-1} in the FTIR spectrum of the complex which is due to the phenolic C– O stretching. The vibrations that confirm the involvement of nitrogen and oxygen atom in chelation with metal ion were also observed. The stretching bands were located at 521 and 401 cm^{-1} which are attributed to the Cu–O and Cu–N bonds with copper (II) ion which is similar to the reported results [25-26].

The thermal decomposition profile of the copper complex and it purity was further studied using the thermogravimetric analysis coupled with Differential thermogravimetric analysis (TGA/DTA). The TGA/DTA curves of the copper complex is shown in Figure 1(b). The TGA results shows that the prepared complex is stable up to 273 °C and displays a single stage decomposition pattern which is supported by the DTA graph on the doted lines. The single decomposition pattern of the metal complex usually arises when there is a high degree of electron delocalization through an intricated system which leads to consistency in bond strength [25, 27]. The mass loss of 68 % in the single stage decomposition stage is in the range of 273 - 465 °C can be ascribed to the loss of ligand moiety with its oxidative degradation to metal oxide.

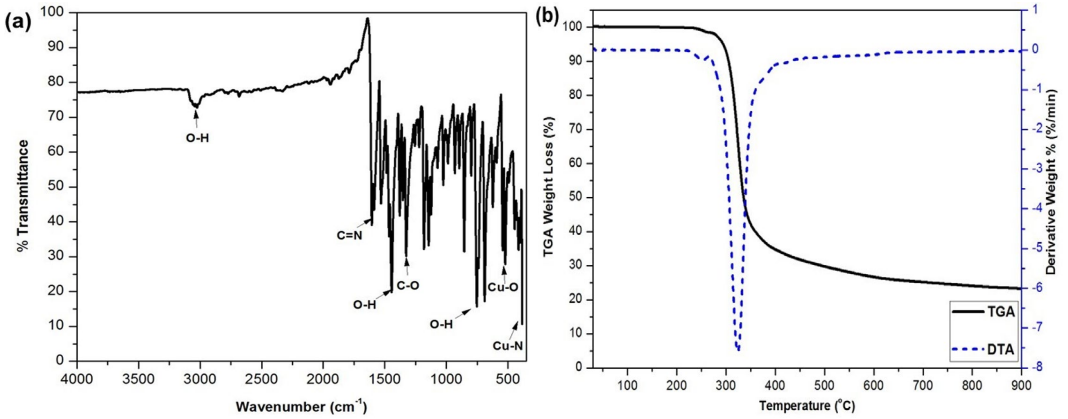

Fig. 1. FTIR spectrum (a) and TGA with DTA curves (b) of the bis(N-benzyl-salicydenaminato) copper (II) complex.

3.2. UV-Vis Spectroscopy and Tauc Plot of CuO Nanoparticles

The absorption spectra and it corresponding Tauc plot and emission spectra of the copper oxide nanoparticles are shown in Figure 2. The absorption spectra (Figure 2(a)) of the copper oxide-TOPO capped nanoparticles synthesized at the temperatures of 120, 180, and 240 °C showed the absorption peaks at 395, 403 and 406 nm as the temperature was increased. The optical bandgap (Eg) of the as synthesized copper oxide nanoparticles was calculated using the Tauc relation [28] given by (1).

$$\alpha h\nu = A(h\nu - E_g)^n \quad (1)$$

where, α is an absorption coefficient, h is Planck constant, ν is the frequency, $h\nu$ is the energy of the incident photon and n is the exponent that determines the type of electronic transition that is causing the absorption which can take the values 0.5, 0.7, 2 or 1.5. CuO and Cu_2O have been reported to be direct band gab semiconductors. From the absorption spectra, the best linear relationship was obtained by plotting $(\alpha h\nu)^n$ (where n = 0.5) against $h\nu$ which is shown in Figure 2(b) and the direct band gap was determined by extrapolating a straight line at $\alpha h\nu = 0$. The direct band gap energies (Eg) of the copper oxide nanoparticles were found to be 3.44, 3.31, and 3.09 eV as the temperature was increased. The Eg values were higher than the theoretical Eg value for the copper oxide bulk material which is 1.85 eV due to the formation of the nano-sized particles which directs to quantum confinement effects [29-30].

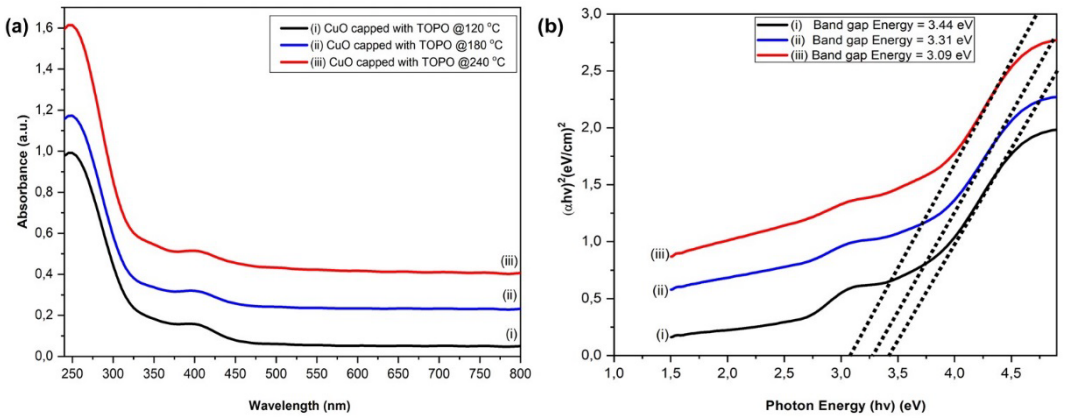

Fig. 2. Absorption (a) and the Variation of $(\alpha h\nu)^2$ vs $h\nu$ (b) of the TOPO capped copper oxide nanoparticles.

3.3. Photoluminescence spectroscopy and X-ray diffraction of CuO nanoparticles

The study of emission properties of the nanoparticles can stipulate an effective information about the quality and purity of the material. Figure 3(a) shows room temperature emission spectra of CuO nanoparticles upon excitation at 400 nm. The spectra of all the copper oxide nanoparticles synthesized at 120, 180, and 240 °C show two emissions bands located between 432-435 nm (most intense band) and 454-456 nm (small band) which were red shifted as the temperature was increased. The most intense emission band in the spectra can be attributed to the recombination of electrons in the conduction band and holes in the valence band [31], whereas the small emission peak might be due to the deep level emission such as oxygen vacancies and Cu interstitials. These results were similar to the reported data [32].

The crystallinity of the synthesized copper oxide nanostructures were studied using the powder X-ray diffraction. The XRD patterns of copper oxide nanoparticles prepared at different temperatures are represented by Figure 3(b). The diffraction pattern of the nanoparticles synthesized at 120 °C show the diffractions peaks at 31.60, 34.65, 36.02, 38.90, 39.21, 45.61, 47.42, 53.97 and 77.25 which are assigned to (110), (002), (-111), (111), (200), (−202), (200), (020) and (004) planes of the monoclinic CuO phase (JCPDS card No. 80-1268). However, the nanoparticles obtained at 180 °C showed diffraction peaks that correspond to both monoclinic CuO and few traces of the face-centred cubic copper phase (JCPDS card number 04-0836). A further increase in temperature to 240 °C, resulted in the formation face-centred cubic metallic copper phase with one peak that correspond to monoclinic CuO phase. The average particle size of the copper oxide nanoparticles was determined by taking the full width at half maximum (FWHM) of the most intense peaks using Debye-Scherrer's formula [33]. The average grain sizes were found to be 3.31, 3.79, and 4.45 nm. The crystalline size calculated from XRD patterns is usually bigger than that of TEM images.

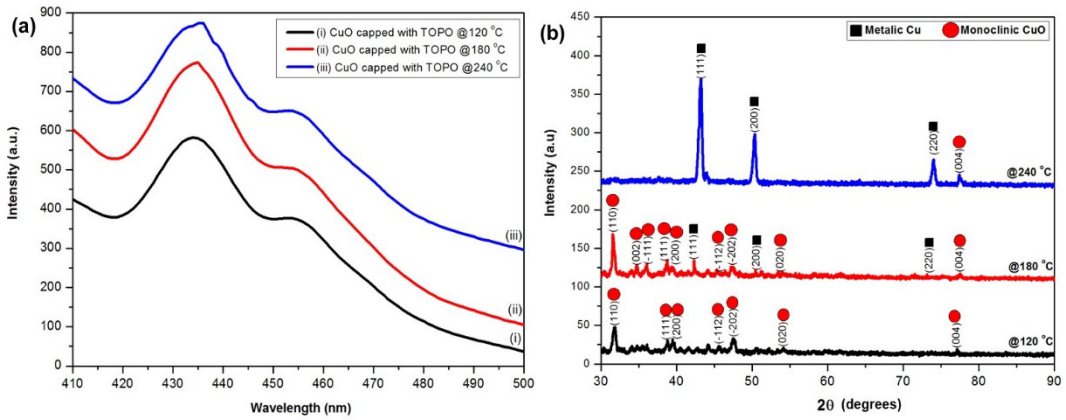

Fig. 3. Emission spectra (a) and X-ray diffraction patterns (b) of the TOPO capped copper oxide nanoparticles.

3.4. Transmitance electron microscopy images of CuO nanoparticles

The morphology and size of the copper oxide nanoparticles was confirmed by transmission electron microscopy (TEM). Fig. 4 shows the TEM images of the nanomaterials that consists of spherical shaped particles which are increasing with the increase in temperature. The images of the copper oxide nanoparticles prepared at 120 and 180 °C (Figure 4(a) & (b)) revealed spherical particles with the average particle diameter of 2.45 ± 0.745 and 3.01 ± 0.873 nm. The nanoparticles synthesized at a temperature of 240 °C (Figure 4(c)) showed the agglomerated spherical particles with the average particle size of 4.13 ± 0.19 nm.

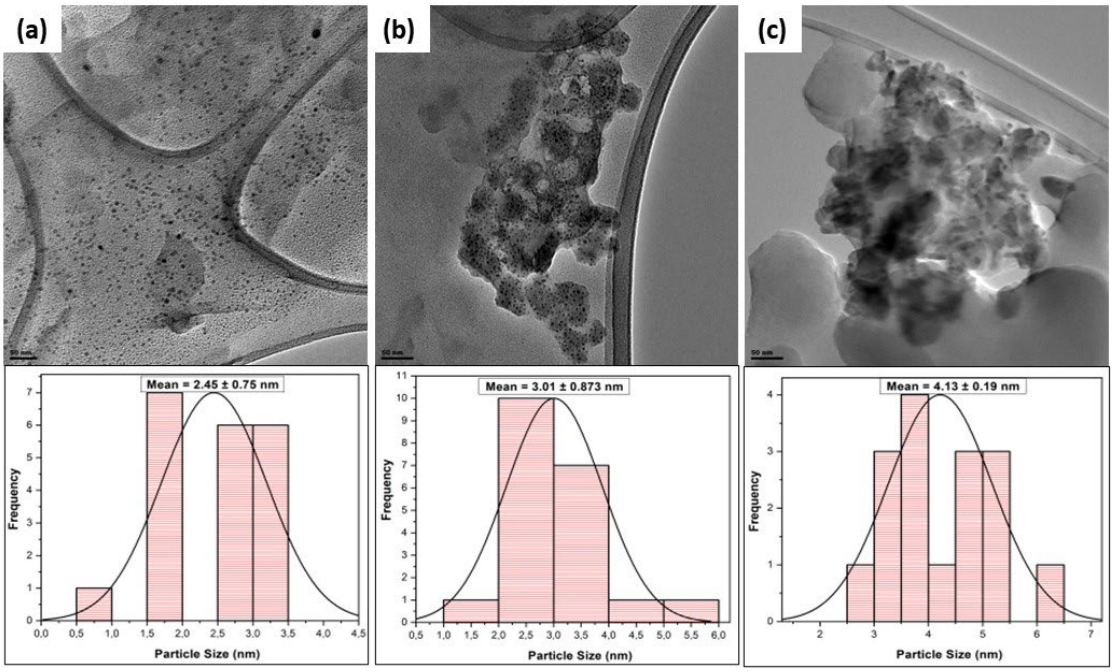

Fig. 4. TEM images and frequency distribution of the TOPO capped copper oxide nanoparticles synthesized at 120 (a), 180 (b) and 240 °C (c).

4. Conclusions

The preparation of *bis*(N-benzyl-salicydenaminato)copper(II) complex has been reported. The synthesis of TOPO capped CuO nanoparticles was done through thermal decomposition method. The absorption and emission spectra of the copper oxide nanoparticles showed that when the temperature was increased, the peaks become red shifted. The XRD patterns of copper oxide nanoparticles synthesized at higher temperature, produced a face-centred cubic metallic copper phase whereas the TEM images revealed the agglomerated spherical particles at high temperature.

Acknowledgements

The authors would like to acknowledge the Vaal University of Technology and National Research Foundation (TTK22051410716: "Thuthuka Grant Holder")) for funding this project.

References

[1] M. Amirnasr, R. Vafazadeh, A. H. Mahmoudkhani, Can. J. Chem., 80, 1196 (2002); https://doi.org/10.1139/v02-122

[2] D. V. Baxter, K. G. Caulton, W. C. Chiang, Polyhedron, 20, 2589 (2001); https://doi.org/10.1016/S0277-5387(01)00825-7

[3] A. Majumder, G. M. Rosair, A. Mallick, N. Chattopadhyay, S. Mitra, Polyhedron, 25, 1753 (2006); https://doi.org/10.1016/j.poly.2005.11.029

[4] T. Akitsu, Y. Einaga, Polyhedron, 25, 1089 (2006); https://doi.org/10.1016/j.poly.2005.07.048

[5] H. Okawa, S. Nakamura, S. Kida, Inorg. Chim. Acta, 120, 185 (1986); https://doi.org/10.1016/S0020-1693(00)86107-1

[6]. M. Enamullah, M. A. Islam, B. A. Joy, G. J. Reiss, Inorganica Chimica Acta, 453, 202 (2006); https://doi.org/10.1016/j.ica.2016.08.013

[7] Y. Wu, H. Q. Yan, M. Huang, B. Messer, J. H. Song, P. Yang, Chem. Eur. J., 8, 1261 (2002).
[8] N. Sundaramurthy, C. Parthiban, International Research Journal of Engineering and Technology, 2, 332 (2015).
[9] M. R. Johan, M. S. Mohd Suan, N. L. Hawari, H. A. Ching, Int. J. Electrochem. Sci., 6, 6094 (2011); https://doi.org/10.1016/S1452-3981(23)19665-9
[10] N. Serin, T. Serin, S. Horzum, Y. Çelik, Semiconductor Science and Technology, 20, 398 (2005); https://doi.org/10.1088/0268-1242/20/5/012
[11] T. Maruyama, Sol. Energy Mater. Sol. Cells, 56, 85 (1998); https://doi.org/10.1016/S0927-0248(98)00128-7
[12] A. A. Eliseev, A. V. Lukashin, A. A. Vertegel, L. I. Heifets, A. I. Zhirov, Y. D. Tretyakov, Materials Research Innovations, 3, 308 (2000); https://doi.org/10.1007/PL00010877
[13] K. Borgohain, J. B. Singh, M. V. Rama Rao, T. Shripathi, S. Mahamuni, Phys Rev. B, 61, 11093 (2000); https://doi.org/10.1103/PhysRevB.61.11093
[14] M. Salavati-Niasari, F. Davar, Mater Lett., 63, 441 (2009); https://doi.org/10.1016/j.matlet.2008.11.023
[15] I. Luna, L. Hilary, A. Chowdhury, M. Gafur, N. Khan, R. Khan, Open Access Library Journal, 2, 1 (2015); https://doi.org/10.4236/oalib.1101409
[16] M. S. Niasari, Z.Fereshteh, F. Davar, Polyhedron, 28, 126 (2009); https://doi.org/10.1016/j.poly.2008.09.027
[17] M. Chandrasekar, M. Subash, S. Logambal, G. Udhayakumar, R. Uthrakumar, C. Inmozhi, Wedad A. Al-Onazi, Amal M. Al-Mohaimeed, Tse-Wei Chen, K. Kanimozhi, Journal of King Saud University - Science, 24, 101831 (2022); https://doi.org/10.1016/j.jksus.2022.101831
[18] K. J. Arun, A. K. Batra, A. Krishna, K. Bhat, M. D. Aggarwal, P. J. Joseph Francis, American Journal of Materials Science, 5, 36 (2015).
[19] A. D. Karthik, K. Geetha, Journal of Applied Pharmaceutical Science, 3, 016 (2013)
[20] T. M. D. Dang, T. T. T. Le, E. Fribourg-Blanc, M. C, Dang, Adv. Nat. Sci: Nanosci. Nanotechnol. 2, 015009 (2011); https://doi.org/10.1088/2043-6262/2/1/015009
[21] C. Wu, B. P. Mosher, T. Zeng, J. Nanopart. Res., 8, 965 (2006); https://doi.org/10.1007/s11051-005-9065-2
[22] T. Akitsu, Y. Einaga, Polyhedron, 25, 1089 (2006); https://doi.org/10.1016/j.poly.2005.07.048
[23] T. Xaba, M. J. Moloto, M. Al-Shakban, M. A. Malik, P. O'Brien, N. Moloto, Materials Science in Semiconductor Processing, 71, 109 (2017); https://doi.org/10.1016/j.mssp.2017.07.015
[24] R. Vafazadeh, V. Hayeri, A. C. Willis, Polyhedron, 29, 1810 (2010); https://doi.org/10.1016/j.poly.2010.02.030
[25] S. S. Swathy, R. Selwin Joseyphus, V. P. Nisha, N. Subhadrambika, K. Mohanan, Arabian Journal of Chemistry, 9, S1847 (2016); https://doi.org/10.1016/j.arabjc.2012.05.004
[26] K. C. Raju, P. K. Radhakrishnan, Synthesis and Reactivity in Inorganic and Metal-Organic Chemistry, 33, 1307 (2007); https://doi.org/10.1081/SIM-120024311
[27] K. Andjelcovie, M. Sumar, I. Ivanovic-Burmazovic, J. Therm. Anal. Cal., 66, 759 (2001); https://doi.org/10.1023/A:1013140021386
[28] J. Tauc, R. Grigorovici, A. Vancu, Physica Status Solidi (b), 15, 627 (1966); https://doi.org/10.1002/pssb.19660150224
[29] H. Wang, J. Z. Xu, J. J. Zhu, H. Y. Chen, J. Cryst. Growth, 244, 88 (2002); https://doi.org/10.1016/S0022-0248(02)01571-3
[30] W. Chen, J. Chen, B. Y. Feng, L. Hong, Q. Y. Chen, L. F. Wu, X. H. Lin, X, H. Xia, Analyst, 137, 1706 (2012); https://doi.org/10.1039/c2an35072f
[31] J. Q. Hu, Y. Bando, Applied Physics Letters, 82, 1401 (2003); https://doi.org/10.1063/1.1558899
[32] A. El-Trass, H. ElShamy, I. El-Mehasseb and M. El-Kemary, Applied Surface Science, 258, 2997 (2012); https://doi.org/10.1016/j.apsusc.2011.11.025

[33] H. Jahangirian, M. H. Shah Ismail, M. D. Jelas Haron, R. Rafiee-Moghaddam, K. Shameli, S. Hosseini, K. Kalantari, R. Khandanlou, E. Gharibshahi, S. Soltaninejad, Digest Journal of Nanomaterials and Biostructures, 8, 1405 (2013).